Millimeter-Wave Ground Based Synthetic Aperture Radar Measurements

Enes YİGİT[1], Atilla UNAL[2], Adem KAYA[2], Sevket DEMİRCİ[1], Harun ÇETİNKAYA[2], Caner ÖZDEMİR[1], Alexey VERTIY[2]

[1]Mersin University, Dept. of Electrical-Electronics Engineering, Yenişehir, 33343 Mersin, Turkey
enesyigit81@mersin.edu.tr, sevdemirci@mersin.edu.tr, cozdemir@mersin.edu.tr

[2] Material Institute, International Laboratory for High Tech. (ILHT), TUBITAK MRC, Gebze, Kocaeli, Turkey
adem.kaya@mam.gov.tr, harun.cetinkaya@mam.gov.tr, atilla.unal@mam.gov.tr , alex.vertii@mam.gov.tr

Abstract

In this study, applications of millimeter wave ground based synthetic aperture radar (GB-SAR) experiments are studied. GB-SAR data collection setup is constructed and GB-SAR measurements of different objects are carried out in the semi-anechoic chamber room. Measurements from an aluminum target and metal pipe targets at the millimeter wave regions are collected by the newly constructed measurement setup. Also, real SAR measurement from metal targets is taken. Then, the millimeter wave GB-SAR images are reconstructed by using a matched filtering type algorithm and the performance of the setup is quantified from the resultant images by evaluating the accuracy and quality metrics.

1. Introduction

Synthetic aperture radar (SAR) is an important remote sensing technique for the monitoring ground and many other applications [1]. Although SAR is generally installed on an airplane or a satellite; recently ground based SAR (GB-SAR) systems have been constructed to give accurate and reliable images of the interested scene [2, 3]. One of the main reasons that the GB-SAR systems are attractive in usage is that they can be constructed using much cheaper electronic equipment and they can operate even at narrow bandwidth of frequencies [4, 5].

Since the down-range resolution in SAR can be achieved by varying the frequency of the transmitted pulse, the improvement of GB-SAR systems have been focused on wideband system production in recent years [6]. Although traditional SAR systems are mainly used at microwave bands, wide frequency bandwidth can easily be exploited at millimeter-wave region thanks to the availability of new technology Vector Network Analyzers (VNA)s at affordable prices. This suitability offers the millimeter resolution capability that can be very crucial in identifying small objects within the scene of interest. Hence, GB-SAR imaging techniques need to be developed for reliable high resolution near field SAR images [7]. For these purpose, millimeter-wave GB-SAR platform is developed and constructed at *the International Laboratory for High Technologies* (ILHT) in *TUBİTAK-Material Institute* in cooperation with *Mersin University* researchers. GB-SAR measurements are collected via the constructed experimental set-up. To accurately form the GB-SAR image of the selected scene, our algorithm based on matched filtering (MF) [8] is utilized.

The organization of the paper is as follows: In section 2, the formulation of the GB-SAR based MF algorithm is given briefly. In section 3, the experimental data collection setup is presented and the results of the millimeter wave GB-SAR measurements are given for three different scenarios. In the last section, issues regarding the effectiveness of the millimeter wave GB-SAR technique are discussed and concluding remarks are given.

2. Matched Filter Algorithm

With the help of experimental data collection setup, obtained GB-SAR data was processed with the MF algorithm [9] which is briefly explained as follows;

The data collection geometry for a monostatic SAR imaging can be described as in Fig. 1. The reflectivity function of the area "A" to be imaged is represented by $\rho(x,y)$. The transmission time of each pulse is denoted by the vector$\{t_n \mid n = 1,2,\dots,N\}$. At nth synthetic aperture point radar which uses stepped frequency, measures the reflection of the targets $S(t_n, f_m)$ given by

$$S(t_n, f_m) = \int_A \rho(x,y).e^{-j2\pi f_m d_n}\, dA \tag{1}$$

where d_n is the two way travel time to the point (x, y) from the nth azimuth sampling position given as

$$d_n = \frac{2.\Delta R(t_n)}{c} \tag{2}$$

where $\Delta R(t_n)$ is a matrix which includes the distances from antenna to the all pixels in the image.

$$\Delta R(t_n) = \frac{2.\sqrt{(X_a - x)^2 + (Y_a - y)^2}}{c} \tag{3}$$

978-1-4244-6051-9/11/$26.00 ©2011 IEEE

where c is a speed of light, X_a and Y_a is location of the antenna with respect to image center. The coordinates of the imaging area are expressed with x and y vectors. $\rho(x,y)$ is the reflectivity of the targets. By taking inverse discrete Fourier transform of Eq. (1), one-dimensional (1D) range profile function for a specific viewpoint is acquired, as shown in below;

$$S(t_n,m) = \int_A \rho(x,y).e^{-j2\pi f_0 d_n}\left[\frac{1}{M}\sum_{k=0}^{M-1} e^{-j2\pi k(\frac{-m}{M}+\Delta f d_n)}\right] dA \quad (4)$$

where $f_0$is the staring frequency of stepped frequency radar. There are M frequency samples so frequency values are represented by the vector$\{f_m \mid m = 1,2,\dots,M\}$. For a point scatterer with reflectivityρ_0, located at (x_0,y_0), 1D range profile function can be written as :

$$S(t_n,m) = \rho_0.e^{-j2\pi f_0 d_n}\left[\frac{1}{M}\sum_{k=0}^{M-1} e^{-j2\pi k(\frac{-m}{M}+\Delta f d_n)}\right] \quad (5)$$

it can be seen from the Eq. (5) that, when $M\Delta f d_n \; is \; equl \; to \; m$, the peak value of the signal occur along the curved path. So the azimuth data line $S(t_n)$, can be obtained by this way;

$$S(t_n) = \rho_0.e^{-j2\pi f_0 d_n} \quad (6)$$

In order to estimate of ρ_0, Eq. (7) have to be multiplied by the Matched Filter function $MF(d_n)$, defined by;

$$MF(d_n) = e^{j2\pi f_0 d_n} \quad (7)$$

To form a matched filtered image $MF(r)$, matched filter function must be applied for an each pixel in the raw data as shown in below.

$$MF(r) = \sum_{n=1}^{N}\sum_{m=1}^{M} S(t_n,f_m)\, e^{j2\pi f_m d_n} \quad (8)$$

3. Measurement Setup and Results

In order to perform the millimeter-wave SAR measurements, the setup shown in Fig. 2 was constructed. The setup consists of Vector Network Analyzer (VNA E8362B), antennas (WR-10 horn antennas), the rail-scanner, and the control computer. VNA is used as the stepped-frequency continuous wave radar (SFCWR) system operating at the frequency band between 75 GHz and 110 GHz. The antennas that were used in the bistatic mode are of pyramidal horn types that has a half-power beam width of 24°at 100 GHz. The rail-scanner, on which all parts of the measurement setup were located, was able to move with a high sensitive constant step size both backward and forward directions. Synchronization between the rail-scanner and VNA were completely automated by using the control computer as illustrated in Fig. 2(a).

Three different experiments were performed for the application of millimeter wave GB-SAR operation. In the first two experiments, undesired signals resulting from ground reflections were eliminated in order to comprehend the influence of millimeter wave on both the range and azimuth resolution. This is because of the fact that the squint angle (shown in Fig. 3(a)) was taken as zero. A real SAR scenario was accomplished in the third experiment.

In the first experiment, two identical metal pipes with 7 cm in diameter were used. As depicted in Figure 1, pipes were positioned at different locations with respect to image center; first pipe was located at ($x = 5\ cm, y = -25\ cm$), and second metal pipe was located at ($x = 0\ cm, y = 10\ cm$). The distance from GB-SAR platform path to the image center was set to 2 m as shown in Figure 1. The length of synthetic aperture was 100 cm for total of 251 discrete measurement points. The frequency of VNA was altered with 50 MHz discrete steps ranging from 75 $GHz\ to$ 81 GHz for a total of 121 frequencies.

At the second experiment an aluminum profile of 4.5 cm x 9 cmx25cm was located at the center of the scene as depicted in Figure 2(c). The distance from GB-SAR platform path to the scene center was set to 1.5 m. The length of the synthetic aperture was 120 cm for total 301 discrete points. The frequency of VNA was changed with 83.33 MHz discrete steps for total 301 points between 75 GHz and 100 GHz.

At the last experiment, two corner reflectors and two aluminum blocks were located at different locations with respect to scene center (see Figure 3(a)). First small corner reflector with a height of 21.5 mm was located at ($x = 0\ cm, y = -35\ cm$), the second corner reflector with a height of 34 mm was positioned at ($x = -5\ cm, y = 0\ cm$), aluminum block of 45x10x119 mm located at ($x = -40\ cm, y = 15\ cm$) and the second aluminum block of 45x10x129 mm placed at ($x = 35\ cm, y = 15\ cm$). The distance from GB-SAR platform path to the scene center was set to3.6m. The length of synthetic aperture was 120 cm for total 301 discrete points. The frequency of VNA was changed with 30 MHz discrete steps for total 201 points from75 GHz to 81 GHz. All data collection parameters used in each experiment is listed in $Table\ I$.

After applying our MF algorithm (MFA), the scattering mechanisms have become more concentrated around the true location of the targets. As shown in Figure 4(a), two major scattering mechanisms are clearly visible from each pipe at the exact locations after applying the MFA. As shown from the Figure 4(b), the aluminum profile is more

accurately imaged with high resolution thanks to the 25 GHz bandwidth at millimeter wave frequencies. It is seen from Fig. 4(c) that the dominant scattering mechanism is occurred from the big corner reflector (at the center of the image). In the SAR applications, the illuminated area of the targets is changed as a result of the height difference of the targets. Hence the reflection from the aluminum block with 129 mm in length (in the right side of Figure 4(c)) is less than other aluminum block with length of 119mm. This mechanism is illustrated in Figure 3(b).

TABLE I. Experimental Parameters

Experiment	Start Frequency (Fstart)	Bandwidth (Bwf)	Number of Stepped Frequency (M)	Synthetic Aperture Length (L)	Squint angle (θ)	# of data collection point (N)	Range resolution $\Delta r = \frac{c}{2.Bwf}$	Azimuth resolution $\Delta a = \frac{\lambda_c . R_0}{L}$
1	75 GHz	6 GHz	121	1 m	0°	251	0.025 m	0.0077 m
2	75 GHz	25 GHz	301	1.2 m	0°	301	0.006 m	0.0043 m
3	75 GHz	6 GHz	201	1.2 m	15°	301	0.025 m	0.0115 m

4. Conclusion

In this work, a millimeter-wave GB-SAR platform is constructed and its imaging performance is investigated thru various experiments. This system uses coherent wide-band millimeter-wave illumination in forming GB-SAR images for different applications. The data collection setup was tested with three different scenarios. A matched filter type algorithm which can be used in near field region is applied to data of GB-SAR measurements. In all of the experiments, targets were accurately detected thanks to the effectiveness of the matched filter algorithm. The wide-band millimeter wave imaging technique mostly removes the effects of speckle noise and gives fairly high resolution (at millimeter lengths) as listed in Table I. Resultant SAR images obtained with our GB-SAR system shows that our measurement can be further developed for the detection and identification of much small objects with high fidelity.

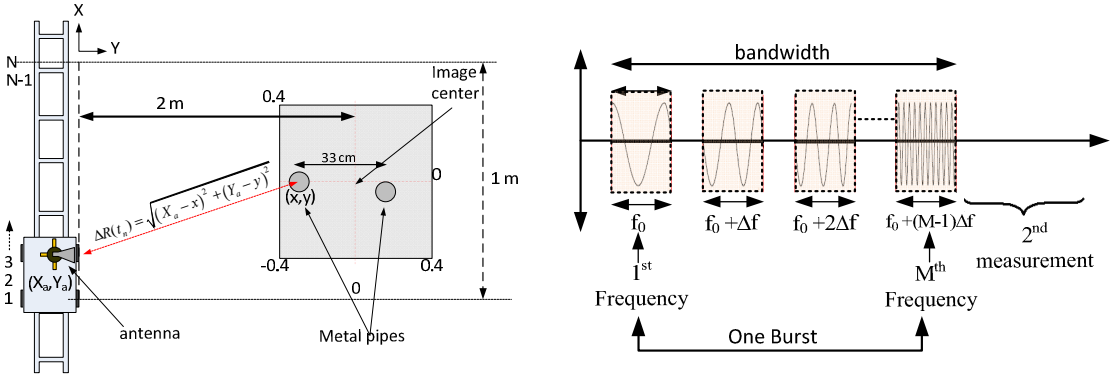

Figure 1. Geometry of scanning techniques of GB-SAR and SFCW radar principle.

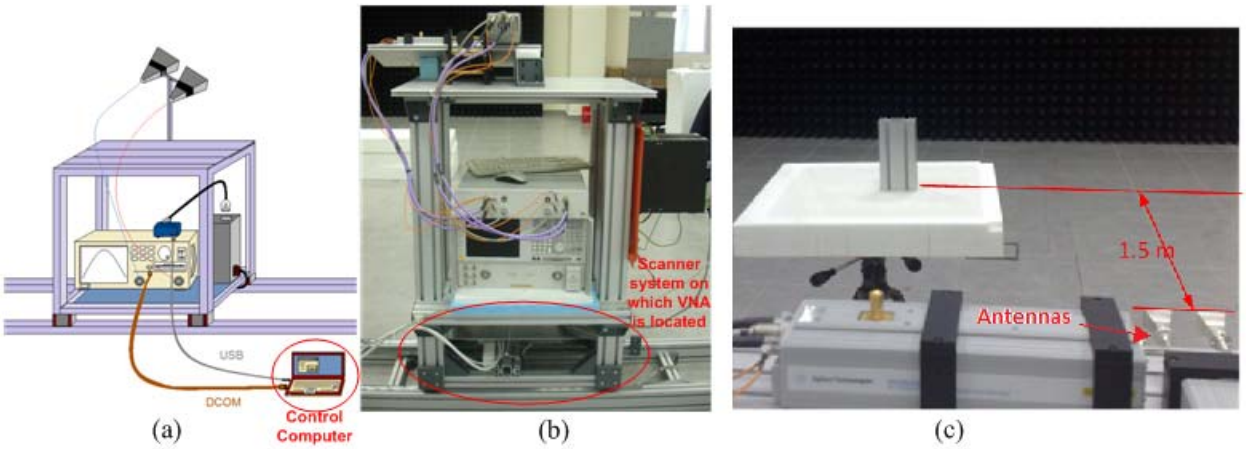

Figure 2. (a) The scheme of millimeter-wave measurement setup. (b) Appearance of the front and back side of the measurement setup. (c) Position of the aluminum profile during the experiment 2.

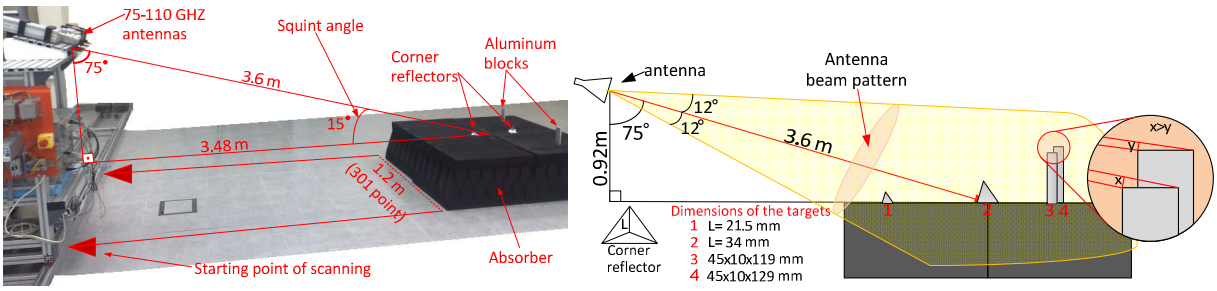

Figure 3. (a) Positions of the targets during the experiment 3, (b) Representation of beam pattern effect

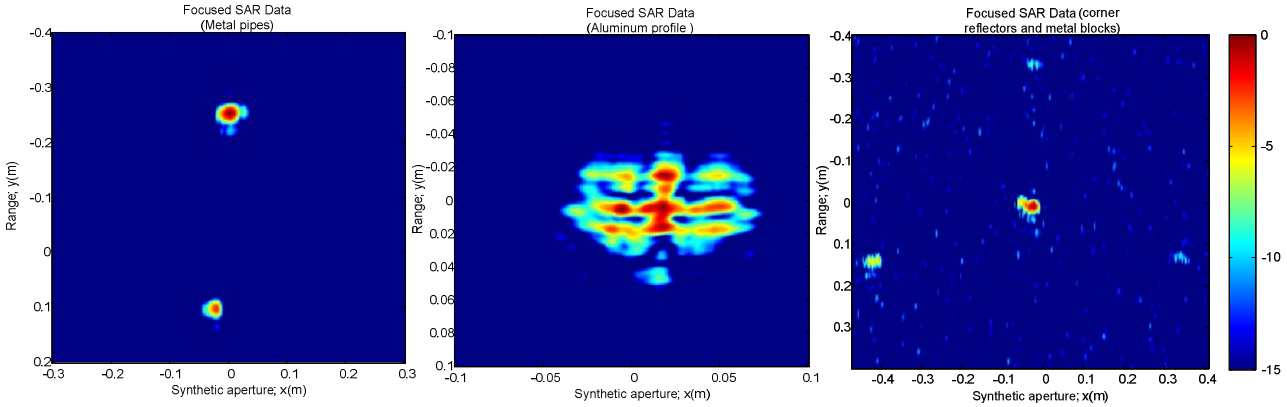

(a) (b) (c)

Figure 4. Focused images of different targets after MF algorithm: (a) metal pipes, (b) aluminum profile, (c) corner reflectors and metal blocks

5. References

1. Özdemir, C., Syntetic Aperture Radar, Editor: K. Chang, *Encyclopedia of RF and Microwave Engineering*, Wiley Interscience, 2005, pp. 5067-5080.

2. Cazzani, L., Colesanti, C., Leva, D., Nesti, G., Prati, C., Rocca, F. and Tarchi, D., "A Ground-Based Parasitic SAR Experiment." IEEE Trans. Geosci. Remote Sensing, **Vol. 38,** No. 5, Sept. 2000, pp. 2132–2141.

3. Cho, B. L., Kong, Y. K., Park, H. G. and Kim, Y. S., "Automobile-Based SAR/InSAR System for Ground Experiments."IEEE Trans. Geosci. Remote Sensing, **Vol. 3,** No. 3, Jul. 2006, pp. 401–405.

4. Koo, V. C., B. K. Chung, and H. T. Chuah, "Development of a ground-based radar for scattering measurements," IEEE Antennas and Propagation Magazine, **Vol. 45**, No. 2, 2003. pp. 36–42.

5. Koo, V. C., B. K. Chung, and H. T. Chuah, "Design and development of a scatterometer system for environmental monitoring," Proceeding of IGARSS 1999 Symposium, Hamburgh,Germany, 1999.

6. Derauw, D., Orban, A. and Barbier, C., "Wide band SAR sub-band splitting and inter-band coherence measurements", Remote Sensing Letters **Vol. 1**, No. 3, Sep. 2010, pp. 133–140.

7. Vertiy, A. A., Gavrilov, S. P., Aksoy, S., Voynovskyy, I. V., Kudelya, A. M., & V. N. Stepanyuk. "Reconstruction of microwave images of the subsurface objects by diffraction tomography and stepped-frequency radar methods," Zarubejnaya Radioelektronika. Uspehi Sovremennoy Radioelektroniki, 2001, pp. 17-52.

8. Soumekh, M., "Synthetic aperture radar signal processing with MATLAB algorithms", Wiley-Interscience, 1999.

9. Gunawardena, A. and Longstaff, D., "A Matched Filter Based Synthetic Aperture Radar (SAR) Algorithm For Stepped Frequency Ground Penetrating Radar", IEEE Radar Conference Int., May. 1995, pp. 239-243.